A fast and accurate global maximum power point tracking controller for photovoltaic systems under complex partial shadings

Adil Atoui[1], Mostefa Kermadi[2], Mohamed Seghir Boucherit[1], Khelifa Benmansour[3], Said Barkat[4], Fethi Akel[5], Saad Mekhilef[2]
[1]Process Control Laboratory, National Polytechnic School, Algiers, Algeria
[2]Power Electronics and Renewable Energy Research Laboratory, Department of Electrical Engineering, University of Malaya, Kuala Lumpur, Malaysia
[3]Polytechnic Military school, UER ELT, Algiers, Algeria
[4]Electrical Engineering Laboratory, Université de M'sila, M'sila, Algeria
[5]Unit de Dveloppement des Equipements Solaires (UDES), Centre de Dveloppement des Energies Renouvelables (CDER), Tipaza, Algeria

Article Info

ABSTRACT

The operating conditions of partially shaded photovoltaic (PV) generators created a need to develop highly efficient global maximum power point tracking (GMPPT) methods to increase the PV system performance. This paper proposes a simple, efficient, and fast GMPPT based on fuzzy logic control to reach the point of global maximum power. The approach measures the PV generator current in the areas where it is almost constant to estimate the local maximums powers and extracts the highest among them. The performance of this method is evaluated firstly by simulation versus four well-known recent methods, namely the hybrid particle swarm optimization, modified cuckoo search, scrutinization fast algorithm, and shade-tolerant maximum power point tracking (MPPT) based on current-mode control. Then, experimental verification is conducted to verify the simulation findings. The results confirm that the proposed method exhibits high performance for complex partial irradiances and can be implemented in low-cost calculators.

Corresponding Author:

Adil Atoui
Process Control Laboratory, National Polytechnic School
Algiers, Algeria
Email: atouiadil@yahoo.fr

1. INTRODUCTION

The power of a photovoltaic generator and its efficiency are strongly linked to the load variation and the climatic conditions [1]–[3]. Various researches have been carried out on this topic to improve the efficiency of this type of renewable source independently of the variation of the irradiance and temperature on one side and load variation on the other side. These researches gave birth to maximum power point tracking (MPPT) methods that track the maximum power point, which have yielded satisfactory results if the generator is exposed to uniform irradiance. Among them, the well-known hill-climbing (HC) [4], incremental conductance (IC), and perturb and observe (P&O), or newer with an adaptive search step like [5], and in [6], the MPPT efficiency is improved by the combination between the algorithm based on fuzzy logic and the IC method, or optimized fuzzy logic control with metaheuristic optimization technique [7] to improve the MPPT efficiency for grid-connected photovoltaic units under uniform irradiances. However, the expansion of solar

energy use in different applications, like solar-powered electrical vehicles [8], wearable technology, backpacks, or larger photovoltaic fields, leads to the exposure of these panels to non-uniform irradiances due to the shadow of objects such as trees, house, clouds, and others. This phenomenon raised the challenge of following the maximum power under partial shading conditions (PSC), which generates the appearance of several local maximum power points (LMPP) [9]. Most of the classical methods failed to achieve the global maximum power point (GMPP) [10]–[13], resulting in a considerable loss of photovoltaic (PV) efficiency.

Recently, several research pieces have addressed the GMPP tracking issue under PSC using metaheuristic methods inspired by nature. They include Jaya algorithm (JA) [14], particle swarm optimization (PSO) [15], cuckoo search (CS) [16], flashing fireflies [17], gray wolf optimization (GWO) [18], flower pollination [19], artificial bee colony (ABC) [20], slap swarm optimization (SSO) [21] or other [11]. These methods converge to the GMPP by following the optimization algorithm based on the random distributions of their particles or populations over the entire search interval. Although this property guarantees to reach the GMPP, their convergence time is slow due to the random nature of the search [13], [22]. Moreover, they generate a big fluctuation when changing irradiance or load [10]. To overcome these two problems, these methods were improved, either by changing parameters like modified cuckoo search (MCS) [23], in which the random parameter Lévy is replaced by a coefficient, or with hybridization like hybrid particle swarm optimization (HPSO) [24], which combines the PSO method and the P&O method. Other hybrid approaches are possible, like the modified genetic algorithm and the firefly algorithm (MGA-FA) [25] and GWO-golden section optimization (GWO-GSO) [26], which combines GWO and GSO. These improvements considerably minimize the convergence time towards the GMPP and minimize the ripples around this point in steady-state. However, the implementation of most of these methods remains complex. This reason leaves the field open to methods based on classical approaches using the shape of the P-V curve to find the GMPP.

The modified IC (MIC) [27] and search-skip-judge (SSJ) global MPPT [10] algorithms are based on the IC method to increase the efficiency of PV under PSC. The downside of MIC is that it fails if there is a complex partial shading containing multiple middle-high peak points (MHP) [12]; it can only detect the first MHP point. The SSJ search time increases when the PV chain contains many modules in series, and the GMPP locates in voltages close to the open-circuit voltage of this chain [10]. The maximum power trapezium (MPT) [28] method limited the search area between V_{min} and V_{max} voltages. It uses the maximum power point current (MPP) under STC conditions (Impp-STC) to determine the minimum voltage V_{min} of the interval of searches, and $V_{max}=0.9V_{oc\text{-}str}$, where $V_{oc\text{-}str}$ is the string open-circuit voltage. Kermadi *et al.* in [13] has developed a scrutinization fast algorithm (SFA) method that uses the concept of MPT combined with the SSJ method to minimize the search areas further and increase PV efficiency. This method gives higher performance than the MPT and flower pollination algorithm (FPA) methods [13]. In Zhou *et al.* [29], proposed a single-sensor GMPPT using the MPT and SSJ skipping mechanisms as in the article [13]. However, the direct current (DC)/DC converter control is based on a single input, the output current sensor, which minimizes the cost of implementation. This method is suitable for a PV system with a fixed voltage at the DC/DC converter output, such as a PV system connected to batteries or the DC bus. It operates the converter DC/DC in continuous conduction mode only. In the article [30], the shade-tolerant (ST) MPPT method uses a current regulator to jump to the left area of the maximum detected point (LHS-MPP) and scans the sites to the right of this point (RHS-MPP) with a fixed step. Although the previous methods, the SFA method in [29], and ST, make jumps, there are still intervals to be scanned by a fixed step, which causes extra time for these methods before reaching the GMPP point. Although the GMPPT methods are many and diverse, it is not easy to determine the most appropriate method that encompasses all performance, ensuring high efficiency, fast-tracking, and a simple implementation on target cards. Consequently, choosing context beforehand is necessary to select a suitable method; this gap motivates the researchers to develop more efficient strategies.

This paper proposes a new method that increases efficiency and speeds up the GMPP tracking while keeping the low calculation burden and implementation simplicity. This method minimizes the scanned intervals by replacing them with a power estimate based on the $0.8V_{oc}$ method, where V_{oc} is the open-circuit voltage of the module. This approach subdivides the voltage of the PV string on the number of modules connected in series and considers that the maximum power point of each zone is in the vicinity of the voltage $0.8V_{oc}$ [31]. The method is built using the fuzzy logic control (FLC) method, which has an adaptive step [3] for local research on the GMPP, which gives it stability at steady-state and high speed to reach this point.

The significant contributions of this work are summarized: i) the proposed method can achieve high efficiency and precision regardless of the type of partial shading, even when there are multiple points of MHP; ii) it improves the GMPPT performance of PV generator under complex shading conditions with a very short time to reach GMPP compared to newer and better-known methods like MCS, SFA, ST, and HPSO; and iii) it is simple, and its implementation needs a target board at minimum performance.

The presented work is subdivided into six sections. In section 2, the PV generator characteristics under the two conditions, uniform irradiance and PSC are shown. Section 3 details the proposed algorithm. Section 4 explains the design and procedure research. Section 5 is devoted to the simulation and experimental results. In the last section, a conclusion is drawn.

2. ELECTRICAL CHARACTERISTICS OF PV GENERATOR

2.1. PV generator under uniform irradiance conditions

The area occupied by a PV generator increases with the number of PV modules connected in series and parallel, increasing the likelihood of its exposure to non-uniform irradiance due to shadow. This phenomenon, called the PSC, changes the behavior of the PV generator. Figure 1 shows three identical modules connected in series with three bypass diodes. The Dp1, Dp2, and Dp3, are connected in parallel with PV1, PV2, and PV3, respectively. These diodes protect the panels from being damaged due to their operation in the hotspot region. In the uniform irradiance, the three modules are exposed to the same irradiance G1=G2=G3; where G1, G2, and G3 are the solar irradiance of PV1, PV2, and PV3 panels, respectively. In this case, the global power of three panels keeps the same form as the case of a single module with a single MPP. However, its voltage increases, thus increasing its maximum power too. Figures 2(a) and (b) represents the PV power and PV current curve of the PV string. The point MPP in Figures 2(a) and (b) corresponds to the voltage V_{m_str} and the current I_{m_str}, which are expressed by (1) and (2) [9], [10]:

$$I_{m_{-str}} \approx 0.9 I_{sc_{-str}} \tag{1}$$

$$V_{m_{-str}} \approx 0.8 V_{oc_{-str}} \tag{2}$$

where I_{sc_str} is the PV string short-circuit current, and V_{oc_str} is the PV string open-circuit voltage.
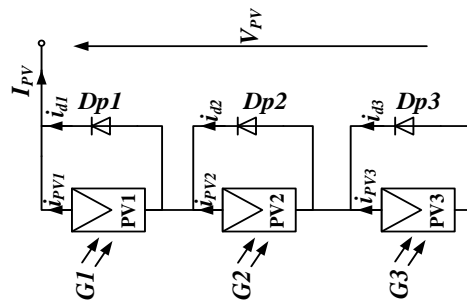
Figure 1. PV generator string with three modules in series
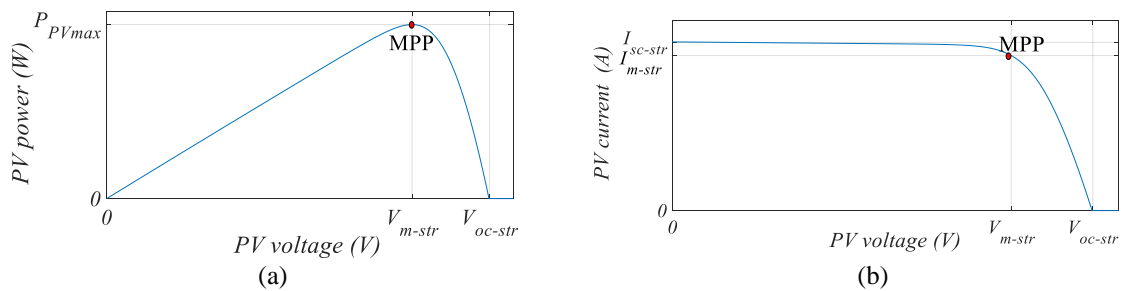
Figure 2. PV string curve under uniform irradiance (a) PV power curve and (b) PV current curve

2.2. PV generator under partial shade conditions

In this case, PV1, PV2, and PV3 are exposed to different irradiance levels, G1, G2, and G3, respectively, where G1>G2>G3. This condition leads to a current curve with three stairs, as shown in Figure 3(a), and a power curve with three local maximum power points (LMPP), as shown in Figure 3(b). The voltage corresponding to the first LMPP (LMPP1) is between 0 and V_{oc1}. Since PV1 is subjected to the

strongest irradiance (G1), only the PV1 panel generates the power, while the other two panels, PV2 and PV3, are short-circuited by diodes Dp2 and Dp3, respectively. In the second stair, where the LMPP2 occurs between the voltages V_{oc1} and V_{oc2}, the two panels, PV1, and PV2, operate with the same current while the PV3 remains short-circuited by the diode Dp3. For the last zone, where the LMPP3 is located between V_{oc2} and V_{oc3}, the three panels PV1, PV2, and PV3 operate with the same current. The current and power shapes are illustrated in Figures 3(a) and (b) respectively. The LMPP2 point in Figure 3(b) is the largest among the other LMPPs, so this point is the GMPP delivered by the PV generator.

The open-circuit voltage of each panel varies slightly with the irradiance variation, so the panels PV1, PV2, and PV3 can be assumed to have the same open-circuit voltage (V_{oc}). Consequently, the voltages V_{oc1}, V_{oc2}, and V_{oc3} shown in Figure 3(a) and (b) can be approximated by $V_{oc1} \approx V_{oc}$, $V_{oc2} \approx 2V_{oc}$, and $V_{oc3} \approx 3V_{oc}$. Therefore, the voltages at LMPPs can also be approximated to $V_{m1} \approx 0.8V_{oc}$, $V_{m2} \approx (1+0.8)V_{oc}$, and $V_{m3} \approx (2+0.8)V_{oc}$ [9]. By similarity, in the general case where there are (Ns) identical series-connected PV modules exposed to partial irradiances, the PV generator current pattern has (Ns) stairs corresponding to the (Ns) area. Let us define a zone as the range of voltages between the two voltage $V_{oc\,(J-1)} = (J-1)V_{oc}$ and the voltage $V_{ocJ} = JV_{oc}$, V_{oc} is the panel open-circuit voltage, J (J=1,2,…, Ns) is the zone number. The shape of the power curve will have an LMPP on each zone, and the LMPP current and voltage in a zone numbered J is given by (3) and (4) [9], [10]:

$$I_{mJ} \approx 0.9 I_{scJ} \tag{3}$$

$$V_{mJ} \approx (J - 1 + 0.8)V_{oc} \tag{4}$$

where I_{mJ} and V_{mJ} are respectively the current and the voltage of the LMPP in zone J, and I_{scJ} the short-circuit current in zone J.
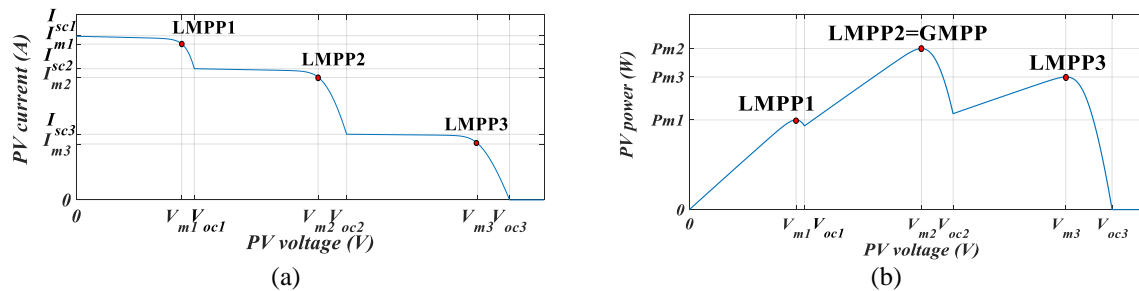
Figure 3. PV string curve under partial shading (a) PV current curve and (b) PV power curve

3. PROPOSED GMPPT METHOD

The proposed method provides simplicity in hardware implementation and increases the speed and precision of reaching the GMPP of the shaded PV system, whatever the complexity of shading conditions. This method is based on the following concepts: i) the subdivision of the PV generator voltage curve into zones, whose number is equal to the panels number in series. Each zone contains a single LMPP; the zone of order n is between the two voltages $(n-1)V_{oc}$ and nV_{oc}, where V_{oc} is the open-circuit voltage of each panel; ii) the current measurement in each zone is performed in the region that is almost constant and close to the short-circuit current I_{sc}; iii) the estimation of the maximum power value at each LMPP point in each zone is based on a technique called the $0.8V_{oc}$ method; and iv) the jump on the zones, which indeed contain an LMPP lower than GMPP (without taking a new current measurement point in these zones). The proposed method flowchart, presented in Figure 4, is divided into several steps.

3.1. Initialization

First, the algorithm is started with an initialization step, which gives the initial values of the indices (J=0, N=1, M=0), that determine the measurement, test zones (the zone (J) is the current area of GMPP. The zone ($J+N$) is the area to compare with the zone (J), M is the jumping index). The PV generator parameters are: the number of panels connected in series (Ns), and the open-circuit voltage V_{oc} of a single generator panel. $Vref_J$ is the voltage that will be given to the DC/DC converter regulator to set the PV generator voltage to this voltage, I_J is the current of the PV generator measured in zone J at the reference voltage $Vref_J$; initially, the algorithm starts with the zone (0), which corresponds to $Vref_{J=0}$=0 and $I_{J=0}$=0.
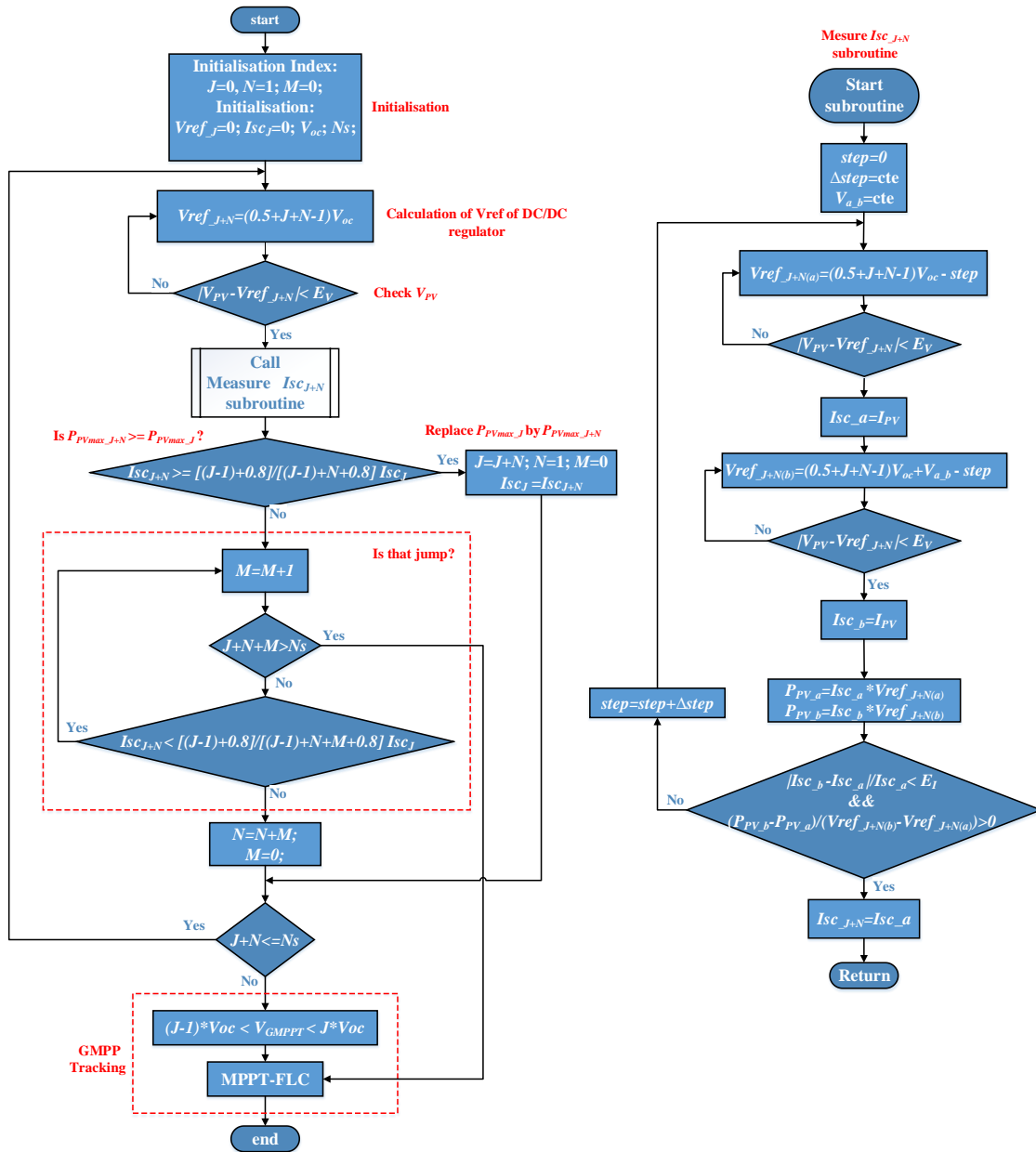
Figure 4. The proposed algorithm flowchart

3.2. Calculation of the PV generator reference voltage to be given to the DC/DC converter regulator

To set the voltage of the PV generator in a zone $(J+N)$ at the desired value, a DC/DC converter regulator connected with the PV generator is used to force the PV voltage to follow its reference $Vref\_{J+N}$ given by (5):

$$Vref\_{J+N} = (0.5 + J + N - 1)V_{oc} \tag{5}$$

The reference $Vref\_{J+N}$ corresponds to the middle of the zone $(J+N)$, which is between the two voltages $(J+N-1)V_{oc}$ and $(J+N)V_{oc,}$ as indicated in Figure 5. At this point, the PV current is almost constant and equals the short-circuit current of the chosen zone, $I_{PV} \approx I_{sc\_J+N}$.

3.3. I_{sc} current measurement

The PV current, corresponding to the reference voltage $Vref\_{J+N}$ in the zone $(J+N)$, must be measured in the right part of the zone, where it is almost constant equal to I_{sc_J+N}. To do this, two measured points, a and b, are considered, at which the voltages are $Vref\_{J+N(a)}=Vref\_{J+N}$ and $Vref\_{J+N(b)}=Vref\_{J+N} +V_{a\_b}$,

where V_{a_b} is the voltage difference between the two points a and b as indicated in Figure 6. To verify that $I_{PV} \approx I_{sc\_J+N}$, two conditions should be satisfied. The first one is:

$$\frac{\Delta P_{PV}}{\Delta V_{PV}} > 0 \tag{6}$$

Resulting in

$$\frac{P_{PV\_b} - P_{PV\_a}}{V_{PV\_b} - V_{PV\_a}} > 0 \tag{7}$$

with $P_{PV\_a} = I_{PV\_a} V_{PV\_a}$ and $P_{PV\_b} = I_{PV\_b} V_{PV\_b}$. The second one is:

$$\frac{|I_{PV\_b} - I_{PV\_a}|}{I_{PV\_a}} < E_I \tag{8}$$

where E_I is the accepted current deviation, if one of the two conditions is not fulfilled, a shift of two points a and b by one step ($\Delta step$) back is performed until reaching the level of I_{sc_J+N}. The choice of E_I is so that the two measurements of the currents I_{PV_a} and I_{PV_b} are taken in the stair between the two currents I_{sc} and I_m of this zone. Therefore, the maximum current deviation of this stair is between the current I_{sc} and I_m, and according to (1), $I_{sc} - I_m$ (1-0.9) $I_{sc} = 0.1 I_{sc}$ by consequence $E_I < 0.1$.
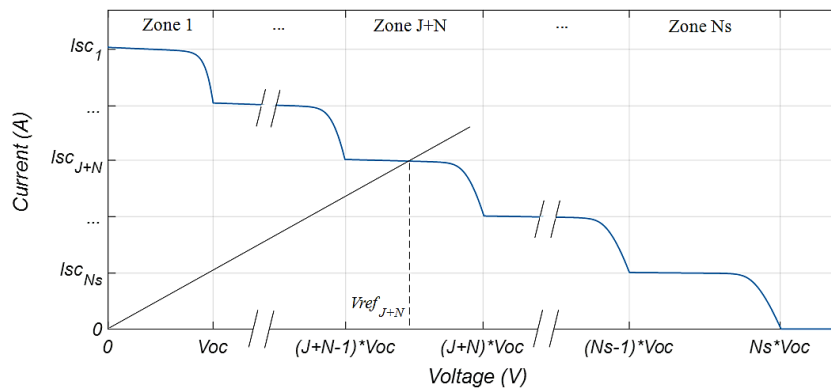
Figure 5. Selection of the reference voltage $Vref\_J+N$ in the middle of the zone $J+N$
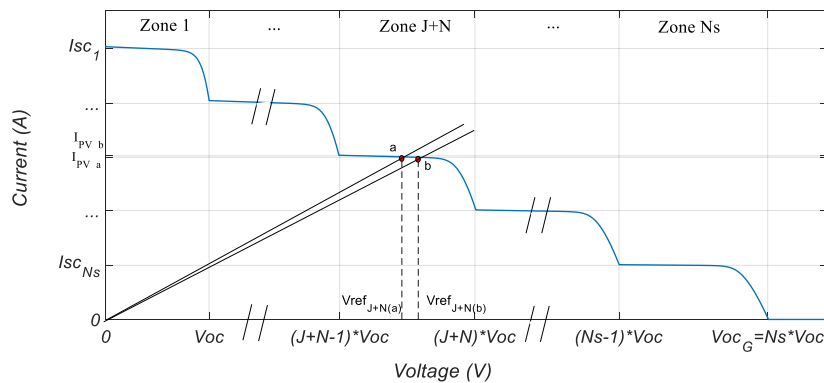
Figure 6. Current measurement procedure

3.4. Comparison between the two estimated powers

The comparison is made between the powers generated in two zones; zone J is assumed to be the current GMPP zone, and zone $(J+N)$ is the new zone to be tested. The two maximum estimated powers of the two zones (J) and ($J+N$) are given by:

$$P_{PV\max J} \approx 0.9 Isc_J [(J-1) + 0.8] V_{oc} \qquad (9)$$

$$P_{PV\max J+N} \approx 0.9 Isc_{J+N} [(J + N - 1) + 0.8] V_{oc} \qquad (10)$$

where P_{PVmaxJ} and $P_{PVmaxJ+N}$ are the maximum estimated powers in zone J and zone $J+N$, respectively. A comparison between the two powers can be established using the following relation:

$$Isc_{J+N} \geq \frac{[(J-1)+0.8]}{[(J+N-1)+0.8]} Isc_J \qquad (11)$$

If the power P_{PVmaxJ} is less than $P_{PVmaxJ+N}$, the latter replaces P_{PVmaxJ} by replacing J by $J+N$ and I_{scJ} by I_{scJ+N}. Otherwise, the power P_{PVmaxJ} is greater than $P_{PVmaxJ+N}$, and the algorithm will go to the jump step.

3.5. The jump to the following zones

In the case where the power $P_{PVmaxJ+N}$ is less than P_{PVmaxJ}, and since the current I_{scJ+N} is greater than the currents of the zones, which follow it, the algorithm compares P_{PVmaxJ} with the power $P_{PVmaxJ+N+M}$ of the zones, which follows the zone $J+N$ using the current I_{scJ+N} without making a new measurement of the current according to the relation:

$$P_{PV\max J+N+M} \approx 0.9 Isc_{J+N} [(J + N + M - 1) + 0.8] V_{oc} \qquad (12)$$

where M is the offset or jumps index; it increments to 1 each time $P_{PVmaxJ} > P_{PVmaxJ+N+M}$. If condition (13) is not satisfied, the algorithm makes a jump without measuring the current on the $J+N+M$ zones.

$$Isc_{J+N} \leq \frac{[(J-1)+0.8]}{[(J+N+M-1)+0.8]} Isc_J \qquad (13)$$

The algorithm repeats the previous steps (without initialization) until the last zone Ns, determined by the number of panels connected in series. After scanning all the zones, zone J, which is between the two voltages $(J-1)V_{oc}$ and the voltage JV_{oc}, is the zone that contains the GMPP.

3.6. Fuzzy logic control based MPPT

This step is to reach the LMPP point of zone J corresponding to the GMPP point. In the literature, there are several methods of following LMPP, and among them, the MPPT is based on fuzzy logic control commonly known as MPPT-FLC [32]. This method does not rely on the mathematical model of the system. This approach uses a variable search step to quickly reach the maximum point and lower the ripple around this point [3], [32]. That increases the PV generator efficiency and robustness in facing load variations and weather conditions.

4.   RESEARCH METHOD

4.1. MATLAB simulation

The block diagram of the system under study is shown in Figure 7. The simulation model is performed using the MATLAB/Simulink SimPowerSystems toolbox environment. The system is composed of a PV string with five series-connected solar panels of type Samsung 250 Watt. Their parameters are shown in Table 1. This string is connected with a DC/DC converter feeding a variable resistance. It is controlled by two proportional integral (PI) controllers in a cascade [33], as shown in Figure 8. The boost converter and PI controller parameters are gathered in Table 1. The control of the PV string is indirectly [2] ensured by the proposed GMPP algorithm, which provides the value of the PV reference voltage (V_{PV_ref}) for the regulator of the DC-DC converter. The latter provides the appropriate duty cycle value to manage the PWM boost converter and set the PV generator voltage (V_{PV}) at its reference value (V_{PV_ref}).

Several irradiance profiles are proposed according to the values of irradiances for the five panels to evaluate the proposed algorithm performance, as shown in Table 2. Figure 9 show the four P-V patterns 1-4 used for the simulation test. This choice is adopted to give different locations for the GMPP. For the first case, all the panels are exposed to the same irradiance level without shading, and in the second case, the GMPP is on the left side of the PV curve. In the third case, the GMPP is in the middle, and in the fourth case, the pattern contains two MHP.

The proposed algorithm is compared with SFA [13] and ST [30], which are considered among the fastest methods based on the exploitation of the P-V pattern. It is also compared with two metaheuristic methods: HPSO [24] and MCS [23]. The three aspects of comparison are: i) the ability to reach the true

GMPP; ii) the convergence time towards the GMPP is defined by the time necessary to achieve the GMPP. It depends on the number of measurement points taken during the search for the GMPP point; and iii) the transient efficiency is calculated using the following relationship [13]:

$$\eta = \frac{\int_{T_0}^{T_f} P_{PV}(t)dt}{\int_{T_0}^{T_f} \int P_{max}} \tag{14}$$

where P_{max} is true GMPP, T_0=0s is the initial time, and T_f =1s is the final time.
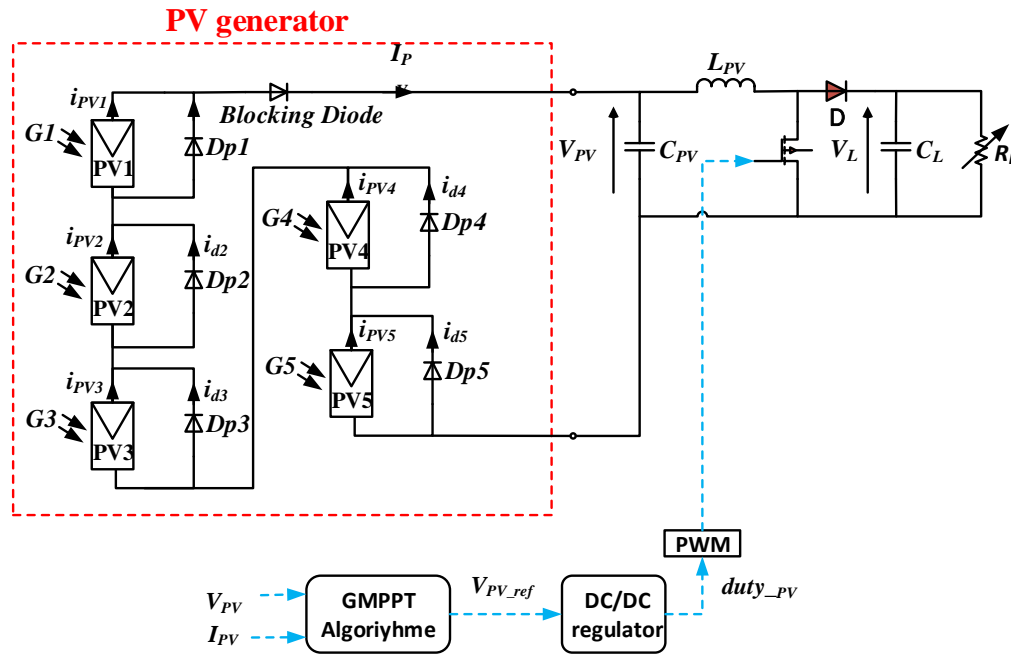
Figure 7. The global scheme of the simulated system

Table 1. Simulation parameters

	Model	Parameters
PV generator	Module: SAMSUNG 250 Watt	P_{max}=250 W, $V_{oc,n}$=37.9V,
	Quantity: five in series	$I_{sc,n}$=8.85A, I_{mpp}=8.24A V_{mpp}=30.3V.
DC-DC converter	Boost DC/DC converter	L_{PV}=5 mH, C_{PV} =200 uF,
		Frequency=20 kHz
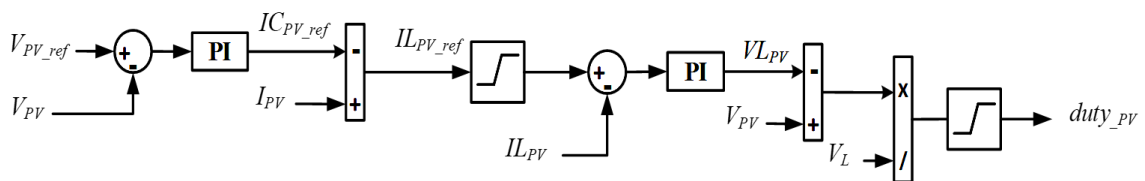
Figure 8. DC/DC regulator

Table 2. Values of the five irradiances for the four patterns

	Pattern 1	Pattern 2	Pattern 3	Pattern 4
G1 (W/m²)	500	950	1000	1000
G2 (W/m²)	500	800	600	800
G3 (W/m²)	500	700	500	450
G4 (W/m²)	500	600	300	390
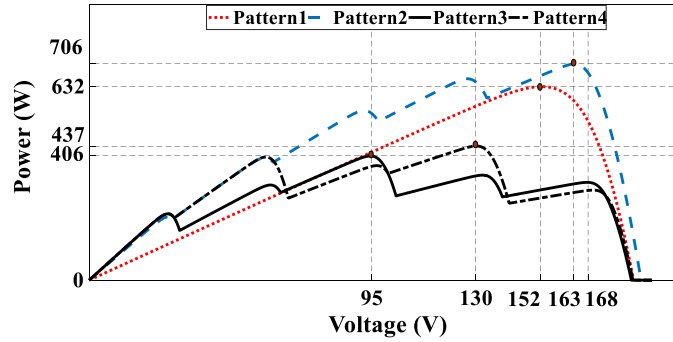
Figure 9. four P-V patterns used in the simulation

4.2. Hardware setup

The experimental verification of the proposed MPPT is ensured using an emulator; it is a controlled DC power supply driven by photovoltaic power profile emulation (PPPE). It emulates the behavior of the PV generator, which is five identical modules connected in series with the same characteristics as those used in the simulation, as shown in Table 1. Three shapes of the shadings are considered, as shown in Figure 10(a)-10(c). These shapes are ensured by PPPE interface software.

The converter used is a buck-boost converter with L=1 mH, C1=1000 uF, and C2=470 uF. The algorithm is implemented on a low-cost and mid-range card (ARDUINO DUE) [34]. Figure 11 represents the overall assembly. The proposed algorithm, which is developed using Simulink, is implemented on an Arduino Due board through the library provided by MATLAB. Its effectiveness was compared with the MCS method chosen among the methods used previously in the simulation, thanks to its simplicity in the face of the limitations of the target card capacities.

(a)

(b)

(c)
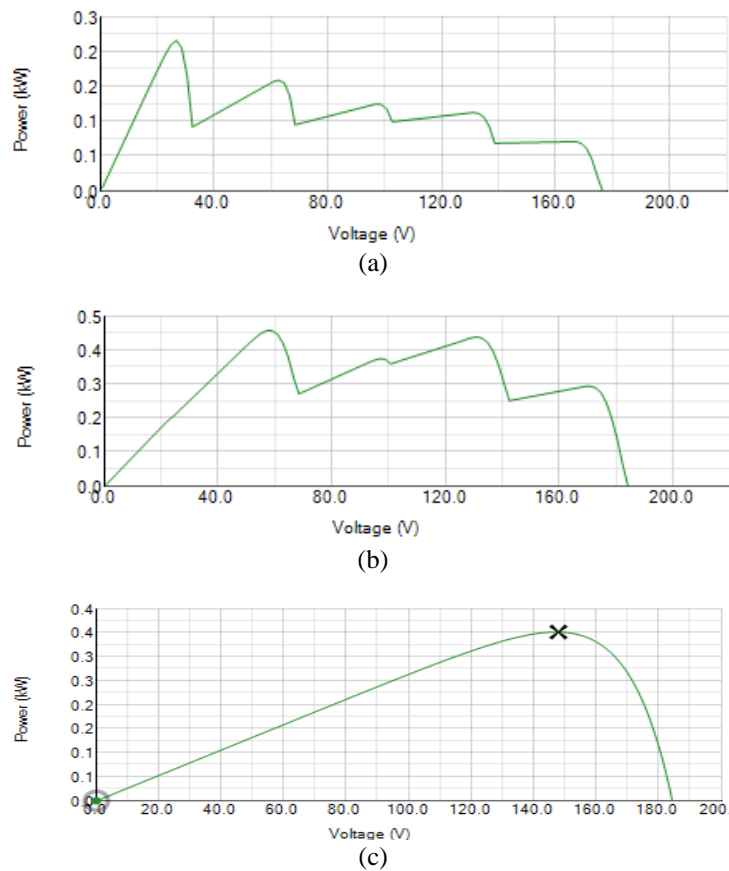
Figure 10. P-V curve, (a) pattern 1, (b) pattern 2, and (c) pattern 3
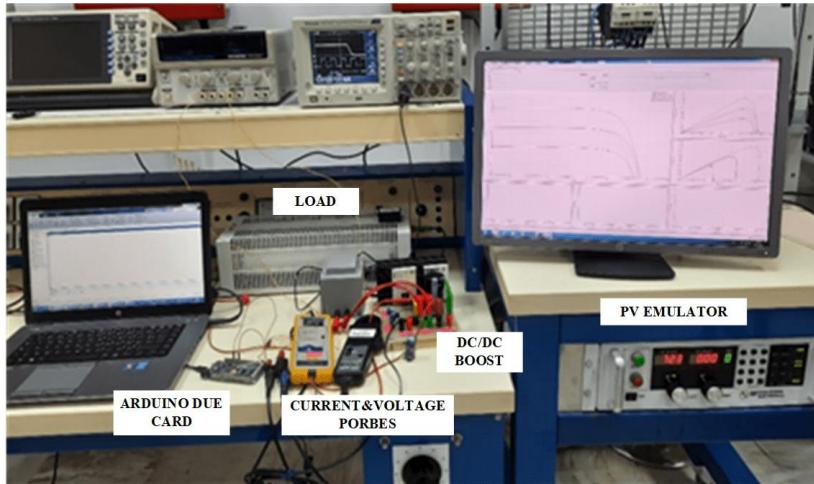
Figure 11. The hardware setup of the MPPT system

5.   RESULTS AND DISCUSSION
5.1. Simulation results

Figures 12-15 illustrate the simulation results for each method for four irradiance models 1-4, with the P-V curve for four patterns in Figures 12(a) to 15(a), PV voltage in Figures 12(b) to 15(b), and PV power in Figures 12(c) to 15(c). Table 3 gives the performances of these methods for the four forms of irradiance. All the simulated methods have reached the true GMPP for the different forms of irradiances, and this is thanks to the process of these methods, which scan the whole range of the PV voltage or make jumps on the zones where there is no GMPP.
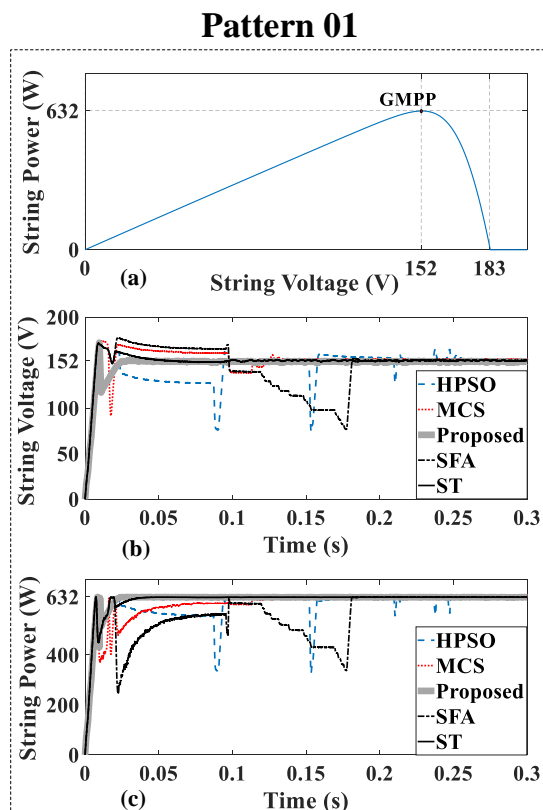
Figure 12. PV curve for Pattern 1 (a) P-V curve,
(b) PV voltage, and (c) PV power
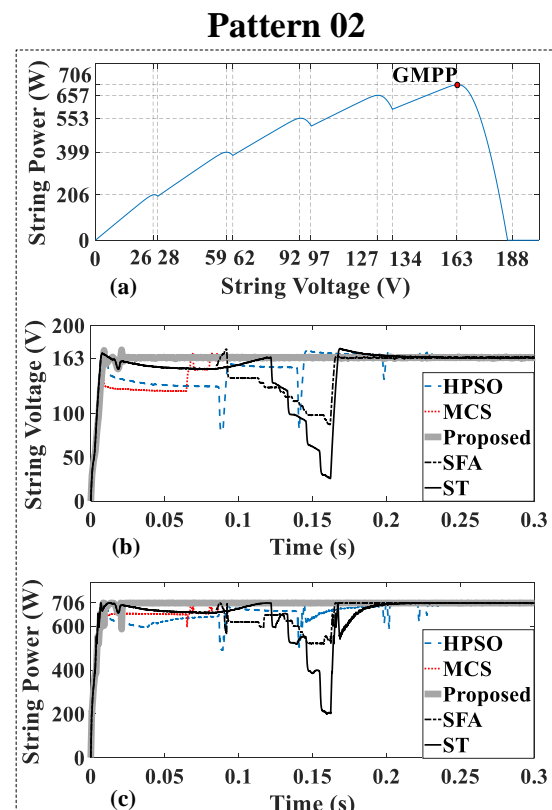
Figure 13. PV curve for Pattern 2 (a) P-V curve,
(b) PV voltage, and (c) PV power

Pattern 03
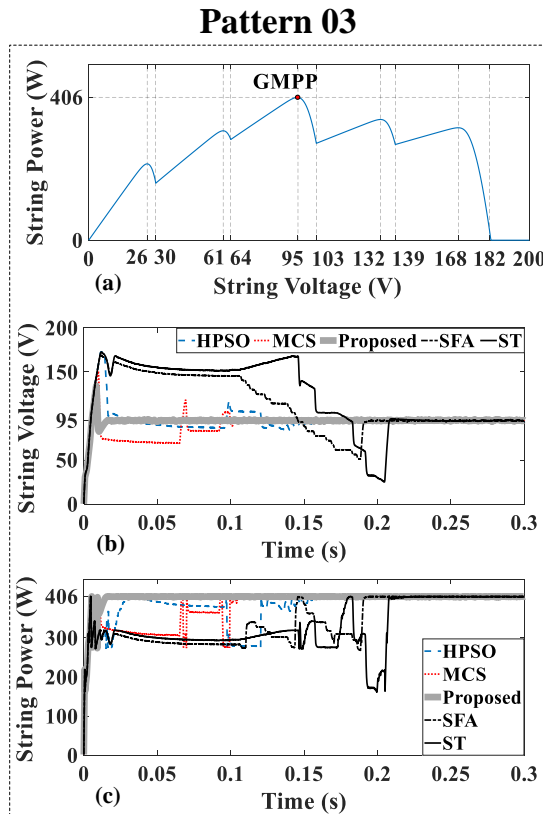
Pattern 04

Figure 14. PV curve for Pattern 3 (a) P-V curve, (b) PV voltage, and (c) PV power
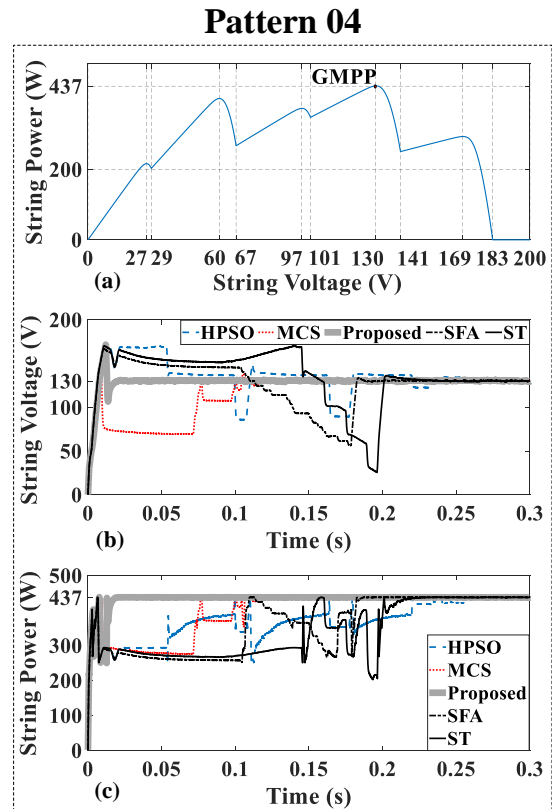
Figure 15. PV curve for Pattern 4 (a) P-V curve, (b) PV voltage, and (c) PV power

Table 3. Performances of the different GMPPT algorithms

| | Pattern 1 | | | Pattern 2 | | | Pattern 3 | | | Pattern 4 | | |
	GMPP (W)	GMPP time (s)	Transient efficiency (%)	GMPP (W)	GMPP time (s)	Transient efficiency (%)	GMPP (W)	GMPP time (s)	Transient efficiency (%)	GMPP (W)	GMPP time (s)	Transient efficiency (%)
HPSO	632.1	0.25	98.23	706	0.24	98.06	406.1	0.16	97.88	437.8	0.27	95.20
MCS	632.1	0.13	98.35	706	0.09	99.05	406.1	0.11	97.76	437.8	0.13	96.96
SFA	632.1	0.18	96.23	706	0.17	98.14	406.1	0.19	95.00	437.8	0.19	94.54
ST	632.1	0.04	99.30	706	0.2	97.49	406.1	0.22	94.19	437.8	0.23	93.29
Proposed	632.1	**0.02**	**99.24**	706	**0.02**	**99.52**	406.1	**0.015**	**99.50**	437.8	**0.02**	**99.47**

The HPSO method had the longest response time due to the number of particles chosen (in this case, there are three particles) and the random choice of the initial positions of these particles. Nevertheless, it keeps high efficiency in all patterns. For example, for pattern 1, the response time of HPSO is 0.25 s with a transition efficiency of 98.23%. On the other hand, the SFA method gives an efficiency of less than 96.23% with a response time of 0.18 s, and this is because the movement of particles in the HPSO is directed towards the GMPP point, which will give a power convergence in the transient state until reaching the GMPP. However, the search is done at predefined intervals in the non-heuristic method (SFA, ST, or proposed one).

The MCS gives high transition efficiency and shorter response time than the HPSO method in the four patterns. The SFA method uses the notion of MPT [28] to limit the search interval between the two voltages V_{min} and V_{max} with $V_{max}=0.9V_{oc\_str}$, V_{oc_str} is the PV string open-circuit voltage, $V_{min}=P_{GMPP}/I_{mpp\_STC}$, where P_{GMPP} is the most considerable PV power over the scanned interval and I_{mpp_STC} is the PV generator current in MPP under STC conditions. Then the V_{min} is the voltage of the point on the power line $P_{MPT}=I_{mpp\_STC} V_{PV}$, which has the power P_{GMPP} as shown in Figure 16. Therefore, V_{min} changes at each new point of P_{GMPP} whose power is greater than the previous one, and the highest V_{min} value corresponds to the maximum power point in the interval [V_{min} V_{max}].

As shown in Table 3, the transition efficiency decreased with decreasing GMPP power of the PV generator due to the widening search interval between V_{min} and V_{max}, as shown in Figure 16. For example, for pattern 2 with P_{GMPP}=706W, its minimum search interval is between V_{max}=168 V and V_{min}=80 V, which

results in an efficiency of 98.14%. On the other hand, in Pattern 3 with P_{GMPP}=406 V, its minimum search interval is between V_{max}=168 V and V_{min}=46 V, which gives an efficiency of 95% less than that provided in pattern 2.

The SI method makes jumps on the zones where the current almost remains fixed to the left of the maximum point LMPP (LHS-MPP) by the mean of the current regulator, which makes the reference current equal to the I_{sc} of this zone with the relation $I_{ref} = I_{sc} = I_{mpp}/0.8$ where I_{mpp} is the LMPP point current reached. While each time, it is necessary to look for the LMPP point in the right zone (RHS-MPP) of this point before making a current jump on the zone (LHS-MPP), as shown in Figure 17. Consequently, the number of (RHS-MPP) zones and their voltage widths will decrease the efficiency of this method and increase its response time. This conclusion is confirmed by the simulation results shown in Table 3. For the four patterns, the initial point is V_0=0.8$V_{oc\text{-}str}$, therefore V_0=187×0.8=150 V, and the widths (L) of the RHS-MPP zones from pattern 1 to pattern 4 indicated by Figures 12-15, are: L_1=2 V, L_2=30 V, L_3=40 V and L_4=43 V; respectively. In contrast to the other previous methods, the proposed method remains very efficient with a very short response time compared to the others for all patterns as long as the number of panels in a series remains fixed (five panels). This feature is owing to its research process, which needs only two measuring points in the middle of each zone n $(n: 1... Ns)$ between two voltages nV_{oc} and $(n+1)V_{oc}$ to estimate the maximum power of this zone and to determine at the end the global maximum power between them.
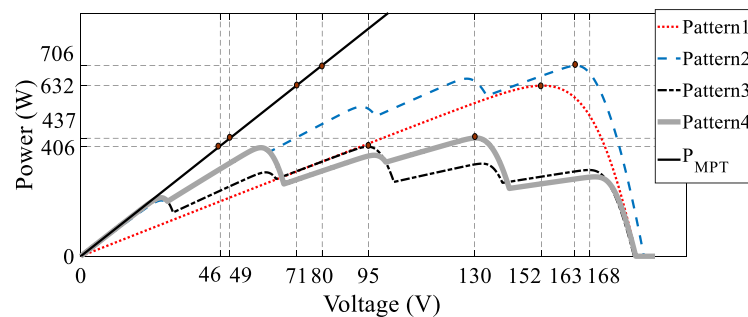
Figure 16. Maximum V_{min} of different patterns
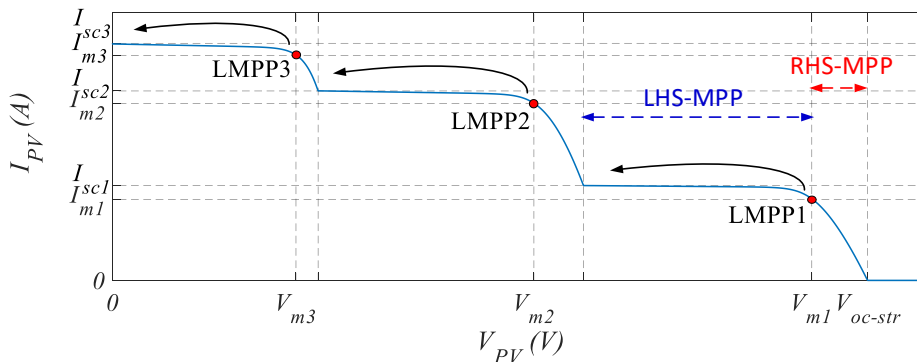
Figure 17. Tracking principle of the ST method

5.2. Experimental results

Figure 18 shows the tracking performance for three patterns with the results obtained for pattern 1 in Figure 18(a), pattern 2 in Figure 18(b), and pattern 3 in Figure 18(c). The interpretation of the results obtained is:

a. Pattern 01: The MCS method missed the GMPP point for this shape because of its process, which is based only on the difference in voltage between its three particles [23]. The proposed method finds the GMPP with a voltage of V_{GMPP}=26 V after a search time that equals t=14.2 s. This is the half of time needed by the MCS method (t=30.2 s), and this is thanks to the procedure of the proposed method, which scans the voltages V1=28 V, V2=62 V and makes a jump on the zones which remain according to the relation (13).

b. Pattern 02: For this pattern, the MCS has found the GMPP point after a time of t=35.2 s. However, the proposed method requires a shorter time to track the GMPP. It requires only t=14.2 s.

c. Pattern 03: Both methods found the GMPP point, which has voltage V_{GMPP}=152 V. But the proposed method is faster with a tracking time of t=8 s than MCS with a tracking time of t=26.8 s.
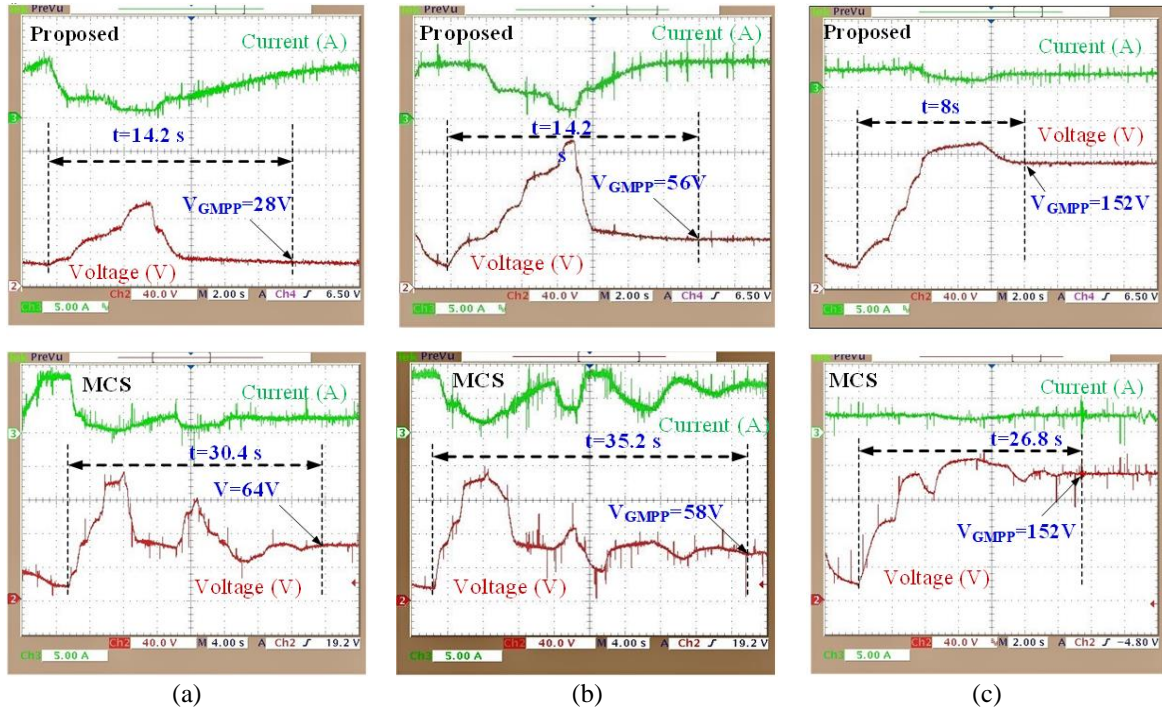
Figure 18. The results obtained, (a) pattern 1, (b) pattern 2, and (c) pattern 3

6. CONCLUSION

In this paper, a simple FLC based approach for global maximum point power GMPP tracking under partial shading conditions is proposed. This approach is based on estimating the maximum power using the principle of the 0.8 V_{oc} method and the current measured in the area where it almost remains constant and equal to the short-circuit current of the shaded PV modules. The proposed method is compared to four recent GMPPT methods; two are heuristic, and the two are based on the PV curve. The comparison was made by examining the ability to achieve the real GMPP, convergence time, and efficiency. The obtained results revealed that the proposed method gives a significant improvement and a higher performance than the other methods regardless of the form and complexity of the partial shading. However, some gaps need to be filled in future work that has not been considered, such as adding a system to differentiate between the shape of the partial shading and the rapid change in irradiance, as well as the type of converter used with its corrector to improve performance further when monitoring the reference voltage.

REFERENCES

[1] Vinod, R. Kumar, and S. K. Singh, "Solar photovoltaic modeling and simulation: As a renewable energy solution," *Energy Reports*, vol. 4, pp. 701–712, Nov. 2018, doi: 10.1016/j.egyr.2018.09.008.

[2] M. Kermadi, S. Mekhilef, Z. Salam, J. Ahmed, and E. M. Berkouk, "Assessment of maximum power point trackers performance using direct and indirect control methods," *International Transactions on Electrical Energy Systems*, vol. 30, no. 10, pp. 1–18, Oct. 2020, doi: 10.1002/2050-7038.12565.

[3] M. Fannakh, M. L. Elhafyani, and S. Zouggar, "Hardware implementation of the fuzzy logic MPPT in an arduino card using a simulink support package for PV application," *IET Renewable Power Generation*, vol. 13, no. 3, pp. 510–518, Feb. 2019, doi: 10.1049/iet-rpg.2018.5667.

[4] S. Motahhir, A. El Hammoumi, and A. El Ghzizal, "The most used MPPT algorithms: Review and the suitable low-cost embedded board for each algorithm," *Journal of Cleaner Production*, vol. 246, Feb. 2020, doi: 10.1016/j.jclepro.2019.118983.

[5] A. Atoui, F. Akel, M. S. Boucherit, and K. Benmansour, "An effective low cost implementation of adaptive fuzzy logic based indirect MPPT method using ARDUINO DUE board," in *Lecture Notes in Networks and Systems*, 2022, vol. 361 LNNS, pp. 285–294, doi: 10.1007/978-3-030-92038-8_29.

[6] M. N. Ali, K. Mahmoud, M. Lehtonen, and M. M. F. Darwish, "An efficient fuzzy-logic based variable-step incremental conductance MPPT method for grid-connected pv systems," *IEEE Access*, vol. 9, pp. 26420–26430, 2021, doi:

10.1109/ACCESS.2021.3058052.

[7]   M. N. Ali, K. Mahmoud, M. Lehtonen, and M. M. F. Darwish, "Promising MPPT methods combining metaheuristic, fuzzy-logic and ANN techniques for grid-connected photovoltaic," *Sensors*, vol. 21, no. 4, Feb. 2021, doi: 10.3390/s21041244.

[8]   A. Sierra Rodriguez, T. Santana, I. MacGill, N. J. Ekins-Daukes, and A. Reinders, "A feasibility study of solar PV-powered electric cars using an interdisciplinary modeling approach for the electricity balance, CO_2 emissions, and economic aspects: The cases of The Netherlands, Norway, Brazil, and Australia," *Progress in Photovoltaics: Research and Applications*, vol. 28, no. 6, pp. 517–532, Jun. 2020, doi: 10.1002/pip.3202.

[9]   R. Ahmad, A. F. Murtaza, H. Ahmed Sher, U. Tabrez Shami, and S. Olalekan, "An analytical approach to study partial shading effects on PV array supported by literature," *Renewable and Sustainable Energy Reviews*, vol. 74, pp. 721–732, Jul. 2017, doi: 10.1016/j.rser.2017.02.078.

[10]   Y. Wang, Y. Li, and X. Ruan, "High-accuracy and fast-speed MPPT methods for PV string under partially shaded conditions," *IEEE Transactions on Industrial Electronics*, vol. 63, no. 1, pp. 235–245, Jan. 2016, doi: 10.1109/TIE.2015.2465897.

[11]   F. Belhachat and C. Larbes, "Comprehensive review on global maximum power point tracking techniques for PV systems subjected to partial shading conditions," *Solar Energy*, vol. 183, pp. 476–500, May 2019, doi: 10.1016/j.solener.2019.03.045.

[12]   M. Kermadi, Z. Salam, J. Ahmed, and E. M. Berkouk, "An effective hybrid maximum power point tracker of photovoltaic arrays for complex partial shading conditions," *IEEE Transactions on Industrial Electronics*, vol. 66, no. 9, pp. 6990–7000, Sep. 2019, doi: 10.1109/TIE.2018.2877202.

[13]   M. Kermadi, Z. Salam, J. Ahmed, and E. M. Berkouk, "A high-performance global maximum power point tracker of PV system for rapidly changing partial shading conditions," *IEEE Transactions on Industrial Electronics*, vol. 68, no. 3, pp. 2236–2245, Mar. 2021, doi: 10.1109/TIE.2020.2972456.

[14]   C. Huang, L. Wang, R. S.-C. Yeung, Z. Zhang, H. S.-H. Chung, and A. Bensoussan, "A prediction model-guided jaya algorithm for the PV system maximum power point tracking," *IEEE Transactions on Sustainable Energy*, vol. 9, no. 1, pp. 45–55, Jan. 2018, doi: 10.1109/TSTE.2017.2714705.

[15]   K. Ishaque and Z. Salam, "A deterministic particle swarm optimization maximum power point tracker for photovoltaic system under partial shading condition," *IEEE Transactions on Industrial Electronics*, vol. 60, no. 8, 2012, doi: 10.1109/TIE.2012.2200223.

[16]   J. Ahmed and Z. Salam, "A maximum power point tracking (MPPT) for PV system using Cuckoo Search with partial shading capability," *Applied Energy*, vol. 119, pp. 118–130, Apr. 2014, doi: 10.1016/j.apenergy.2013.12.062.

[17]   K. Sundareswaran, S. Peddapati, and S. Palani, "MPPT of PV systems under partial shaded conditions through a colony of flashing fireflies," *IEEE Transactions on Energy Conversion*, vol. 29, no. 2, pp. 463–472, 2014, doi: 10.1109/TEC.2014.2298237.

[18]   S. Mohanty, B. Subudhi, and P. K. Ray, "A new MPPT design using grey wolf optimization technique for photovoltaic system under partial shading conditions," *IEEE Transactions on Sustainable Energy*, vol. 7, no. 1, pp. 181–188, Jan. 2016, doi: 10.1109/TSTE.2015.2482120.

[19]   J. Prasanth Ram and N. Rajasekar, "A novel flower pollination based global maximum power point method for solar maximum power point tracking," *IEEE Transactions on Power Electronics*, vol. 32, no. 11, pp. 8486–8499, Nov. 2017, doi: 10.1109/TPEL.2016.2645449.

[20]   K. Sundareswaran, P. Sankar, P. S. R. Nayak, S. P. Simon, and S. Palani, "Enhanced energy output from a pv system under partial shaded conditions through artificial bee colony," *IEEE Transactions on Sustainable Energy*, vol. 6, no. 1, pp. 198–209, Jan. 2015, doi: 10.1109/TSTE.2014.2363521.

[21]   A. F. Mirza, M. Mansoor, Q. Ling, B. Yin, and M. Y. Javed, "A salp-swarm optimization based MPPT technique for harvesting maximum energy from PV systems under partial shading conditions," *Energy Conversion and Management*, vol. 209, Apr. 2020, doi: 10.1016/j.enconman.2020.112625.

[22]   J. Ahmed and Z. Salam, "A critical evaluation on maximum power point tracking methods for partial shading in PV systems," *Renewable and Sustainable Energy Reviews*, vol. 47, pp. 933–953, Jul. 2015, doi: 10.1016/j.rser.2015.03.080.

[23]   B.-R. Peng, K.-C. Ho, and Y.-H. Liu, "A novel and fast MPPT method suitable for both fast changing and partially shaded conditions," *IEEE Transactions on Industrial Electronics*, vol. 65, no. 4, pp. 3240–3251, 2018, doi: 10.1109/TIE.2017.2736484.

[24]   K. L. Lian, J. H. Jhang, and I. S. Tian, "A maximum power point tracking method based on perturb-and-observe combined with particle swarm optimization," *IEEE Journal of Photovoltaics*, vol. 4, no. 2, pp. 626–633, Mar. 2014, doi: 10.1109/JPHOTOV.2013.2297513.

[25]   Y.-P. Huang, X. Chen, and C.-E. Ye, "A hybrid maximum power point tracking approach for photovoltaic systems under partial shading conditions using a modified genetic algorithm and the firefly algorithm," *International Journal of Photoenergy*, pp. 1–13, 2018, doi: 10.1155/2018/7598653.

[26]   J. Y. Shi *et al.*, "Dual-algorithm maximum power point tracking control method for photovoltaic systems based on grey wolf optimization and golden-section optimization," *Journal of Power Electronics*, vol. 18, no. 3, pp. 841–852, 2018, doi: 10.6113/JPE.2018.18.3.841.

[27]   K. S. Tey and S. Mekhilef, "Modified incremental conductance algorithm for photovoltaic system under partial shading conditions and load variation," *IEEE Transactions on Industrial Electronics*, vol. 61, no. 10, pp. 5384–5392, 2014, doi: 10.1109/TIE.2014.2304921.

[28]   A. M. S. Furtado, F. Bradaschia, M. C. Cavalcanti, and L. R. Limongi, "A reduced voltage range global maximum power point tracking algorithm for photovoltaic systems under partial shading conditions," *IEEE Transactions on Industrial Electronics*, vol. 65, no. 4, pp. 3252–3262, Apr. 2018, doi: 10.1109/TIE.2017.2750623.

[29]   G. Zhou, Q. Bi, Q. Tian, M. Leng, and G. Xu, "Single sensor based global maximum power point tracking algorithm of pv system with partial shading condition," *IEEE Transactions on Industrial Electronics*, vol. 69, no. 3, pp. 2669–2683, Mar. 2022, doi: 10.1109/TIE.2021.3066920.

[30]   S. Hosseini, S. Taheri, M. Farzaneh, and H. Taheri, "A high-performance shade-tolerant MPPT based on current-mode control," *IEEE Transactions on Power Electronics*, vol. 34, no. 10, pp. 10327–10340, Oct. 2019, doi: 10.1109/TPEL.2019.2894528.

[31]   A. Kouchaki, H. Iman-Eini, and B. Asaei, "A new maximum power point tracking strategy for PV arrays under uniform and non-uniform insolation conditions," *Solar Energy*, vol. 91, pp. 221–232, May 2013, doi: 10.1016/j.solener.2013.01.009.

[32]   T. Esram and P. L. Chapman, "Comparison of photovoltaic array maximum power point tracking techniques," *IEEE Transactions on Energy Conversion*, vol. 22, no. 2, pp. 439–449, 2007, doi: 10.1109/TEC.2006.874230.

[33]   A. Choudar, D. Boukhetala, S. Barkat, and J.-M. Brucker, "A local energy management of a hybrid PV-storage based distributed generation for microgrids," *Energy Conversion and Management*, vol. 90, pp. 21–33, Jan. 2015, doi: 10.1016/j.enconman.2014.10.067.

[34]   "Arduino," *Arduino official website*. https://www.arduino.cc/ (accessed Jun. 01, 2021).

BIOGRAPHIES OF AUTHORS

Adil Atoui was born in M'sila, Algeria, in 1984. In 2008, he received an engineering degree in electrical engineering from the University of M'sila, Algeria. In 2012, he graduated M.Sc. degree in electrical engineering from the National Polytechnic School, Algiers, Algeria. Currently, he is a Ph.D. student at the National Polytechnic School. Since 2015, he is presently working as an assistant professor at the National Maritime Superior School, Tipaza, Algeria. His current research interests include power electronics, renewable energies, artificial intelligence, energy, power management system, embedded system, and microgrids. He can be contacted at email: atouiadil@yahoo.fr.

Mostefa Kermadi (M'20) received Engineering (Dipl. Ing.) and Master degree in Control Engineering in 2012, and PhD in Automatic Control in 2018, all from National Polytechnic School (ENP) of Algiers, Algeria. During his PhD work, he was a visiting researcher at the Centre of Electrical Energy Systems (CEES), Universiti Teknologi Malaysia (UTM), Malaysia, from December 2016 to July 2018. He is currently a Post-doctoral Research Fellow with the Power Electronics and Renewable Energy Research Laboratory (PEARL), Department of Electrical Engineering, University of Malaya, Malaysia. His research interests include predictive control of power converters, power conversion and management in renewable energy systems. He can be contacted at email: mostefa@um.edu.my.

Mohamed Seghir Boucherit was born in 1954 in Algiers. He received the Engineer degree in Electrotechnics, the Magister degree and the Doctorat d'Etat (Ph.D. degree) in Electrical Engineering, from the Ecole Nationale Supérieure Polytechnique, of Algiers, Algeria, in 1980, 1988 and 1995 respectively. Upon graduation, he joined the Electrical Engineering Department of Ecole Nationale Polytechnique. He is a Professor, Head of the Industrial systems and Diagnosis research team of the Process Control Laboratory and his research interests are in the area of Electrical Drives, Process Control Applications, and Diagnosis. He can be contacted at email: ms_boucherit@yahoo.fr.

Khelifa Benmansour received his BEng (Hons) degree in Power Systems Engineering and his Master's degree in Electrical Engineering from the Ecole Nationale Polytechnique, (ENP, EMP) Algiers, Algeria, in 1997 and 1999, respectively. He is currently a Professor at the University of Medea, (Algeria). He received his PhD degree in Control Systems Engineering from Ecole Nationale Polytechnique ENP, Algeria in 2006. His main research interest includes the control of nonlinear systems and sliding mode control and observers, fault detection and machine speed sensors, drives and the analysis and multi-cellular converters and hybrid systems. He can be contacted at email: kh.benmansour@gmail.com.

Said Barkat received the Ph.D. degree in electrical engineering from the National Polytechnic School of Algiers, Algeria, in 2008. In 2000, he joined the Faculty of Technology at M'sila University, Algeria, where he is currently a full professor with the Electrical Engineering Department. His research interests include renewable energy conversion, power electronics, and advanced control theory and applications. He can be contacted at email: said.barkat@univ-msila.dz.

Fethi Akel [ID] [SC] received the Magister and Doctorate degrees in Electrical Engineering in 2009 and 2017 respectively, from the Polytechnic Military School (ex: ENITA) and National Polytechnic School (ENP), Algiers, Algeria, respectively. Currently, he is a full-time researcher with Solar Equipments Development Unit (UDES)/Renewable Energy Development Center (CDER). He has authored many published articles in international journals and conference proceedings in the area of power control systems. His research interests are focused on designing control systems and implementing power converters-based renewable energy systems. He is currently working on advanced renewable energy-based generators and energy management systems for micro-grids and future smart grids. He can be contacted at email: akel.fethielt@gmail.com.

Saad Mekhilef [ID] [SC] is an IEEE and IET Fellow. He is a Distinguished Professor at the School of Science, Computing and Engineering Technologies, Swinburne University of Technology, Australia, and an Honorary Professor at the Department of Electrical Engineering, University of Malaya. He authored and co-authored more than 500 publications in academic journals and proceedings and five books with more than 34,000 citations, and more than 70 Ph.D. students graduated under his supervision. He serves as an editorial board member for many top journals such as IEEE Transaction on Power Electronics, IEEE Open Journal of Industrial Electronics, IET Renewable Power Generation, Journal of Power Electronics, and International Journal of Circuit Theory and Applications. Prof. Mekhilef has been listed by Thomson Reuters (Clarivate Analytics) as one of the Highly Cited (World's Top 1%) engineering researchers in the world in 2018,2019, 2020, and 2021. He is actively involved in industrial consultancy for major corporations in the Power Electronics and Renewable Energy projects. His research interests include power conversion techniques, control of power converters, maximum power point tracking (MPPT), renewable energy, and energy efficiency. He can be contacted at email: saad@um.edu.my.